

FTIR and Fluorescence Studies of Interactions of Synaptic Fusion Proteins in Polymer-Supported Bilayers[†]

Jiang Zhao and Lukas K. Tamm*

Department of Molecular Physiology and Biological Physics, University of Virginia,
Health System, P.O. Box 800736, Charlottesville, Virginia 22908-0736

Received July 11, 2002. In Final Form: October 26, 2002

Single planar phospholipid bilayers supported on soft polymer (poly(ethylene glycol), PEG) cushions have served as useful models for biological membranes. Integral membrane proteins can be successfully reconstituted in covalently tethered PEG3400-supported bilayers (=DPS-supported bilayers) where they bind their natural ligands as in biological membranes and where they exhibit almost normal physiological lateral diffusion properties. Here, we have characterized DPS-supported bilayers by polarized attenuated total reflection Fourier transform infrared (ATR-FTIR) spectroscopy. The bilayers are not significantly perturbed by the polymer, and the vibrational bands of PEG do not interfere with the interpretation of several major lipid and protein bands, clearing the way to study protein secondary structure and lipid–protein interactions in DPS-supported lipid bilayers by ATR-FTIR spectroscopy. We have also reconstituted v- and t-SNARE proteins and formed membrane-bound SNARE complexes in this model system. Membrane-bound v-SNAREs (VAMP2 or synaptobrevin2) are unstructured, and membrane-bound t-SNAREs (syntaxin1A/SNAP-25) are predominantly α -helical. v-SNAREs, but not t-SNAREs, exchange readily between the polymer-supported bilayer and lipid vesicles in solution, suggesting that v-SNAREs do not possess a classical stable transmembrane anchor at their C-terminus. SNARE complex formation between the polymer-supported membrane and lipid vesicles does not induce detectable additional α -helical secondary structure in this system.

Introduction

Supported lipid bilayer membranes¹ have gained wide application in fundamental and applied membrane research. Investigators have used them to study lipid–protein interactions,^{2–4} domain formation in membranes,^{5–7} ion channel conductance across membranes,^{8,9} structures of membrane-bound proteins,^{10,11} interactions between supported model membranes and cells,^{12,13} matrixes for membrane-based biosensors,^{14,15} and many other applications. A common problem of supported bilayer technology

has been the relatively narrow water-filled gap between the bilayer and the support.^{1,16} This gap is not wide enough to accommodate large integral membrane proteins that protrude more than about 1 nm from the surface of the substrate-exposed inner lipid monolayer. To alleviate this problem, several groups have started to support lipid bilayers on soft polymer cushions that are intercalated between the hard inorganic substrate and the lipid bilayer.^{17–19} To provide as close a biological environment as possible, the polymer must be readily miscible with water and should be soft, that is, extendable and compressible, in an aqueous buffered saline at around neutral pH and ~ 0.15 M ionic strength. The polymer must also support the normal planar lipid bilayer structure over long distances (at least several hundred microns), allow for long-range translational lipid diffusion as in a normal bilayer in the liquid-crystalline phase (lateral diffusion coefficient, $\sim 1 \mu\text{m}^2/\text{s}$), and, most critically, should permit lateral diffusion of functionally incorporated integral membrane proteins.

Our approach to this problem has been to construct polymer-supported bilayers on cushions of poly(ethylene glycol).²⁰ Poly(ethylene glycol) (PEG) does not interact with quartz, glass, silicon oxide, lipids, or proteins. It forms random coils in water and, therefore, appears to be a good choice for a polymer as a substrate to support lipid bilayers that should serve as models for biological membranes. However, for the same reasons, PEG does not stick by itself to hydrophilic surfaces and, therefore, is not suitable

* To whom correspondence should be addressed. Tel: (434) 982-3578. Fax: (434) 982-1616. E-mail: lkt2e@virginia.edu.

[†] Part of the *Langmuir* special issue entitled The Biomolecular Interface.

- (1) Tamm, L. K.; McConnell, H. M. *Biophys. J.* **1985**, *47*, 105–113.
- (2) Frey, S.; Tamm, L. K. *Biophys. J.* **1991**, *60*, 922–930.
- (3) Maierhofer, A. P.; Bucknall, D. G.; Bayerl, T. M. *Biophys. J.* **2000**, *79*, 1428–1437.
- (4) Han, X.; Tamm, L. K. *Proc. Natl. Acad. Sci. U.S.A.* **2000**, *97*, 13097–13102.
- (5) Dietrich, C.; Bagatolli, L. A.; Volovky, Z. N.; Thompson, N. L.; Levi, M.; Jacobson, K.; Gratton, E. *Biophys. J.* **2001**, *80*, 1417–1428.
- (6) Groves, J. T.; Boxer, S. G.; McConnell, H. M. *Proc. Natl. Acad. Sci. U.S.A.* **1998**, *95*, 935–938.
- (7) Bieri, C.; Ernst, O. P.; Heyse, S.; Hofmann, K. P.; Vogel, H. *Nat. Biotechnol.* **1999**, *17*, 1105–1108.
- (8) Stelzle, M.; Weismüller, G.; Sackmann, E. *J. Phys. Chem.* **1993**, *97*, 2974–2981.
- (9) Fromherz, P.; Kiessling, V.; Kottig, K.; Zeck, G. *Appl. Phys. A* **1999**, *69*, 571–576.
- (10) Yang, J.; Tamm, L. K.; Tillack, T. W.; Shao, Z. *J. Mol. Biol.* **1993**, *229*, 286–290.
- (11) Czajkowsky, D.; Iwamoto, H.; Cover, T.; Shao, Z. *Proc. Natl. Acad. Sci. U.S.A.* **1999**, *96*, 2001–2006.
- (12) Brian, A. A.; McConnell, H. M. *Proc. Natl. Acad. Sci. U.S.A.* **1984**, *81*, 6159–6163.
- (13) Grakoui, A.; Bromley, S. K.; Sumen, C.; Davis, M. M.; Shaw, A. S.; Allen, P. M.; Dustin, L. M. *Science* **1999**, *285*, 221–226.
- (14) Cornille, B. A.; Braach-Maksyvtis, V. L. B.; King, L. G.; Osman, P. D. J.; Raguse, B.; Wiczorek, L.; Pace, R. J. *Nature* **1997**, *387*, 580–583.
- (15) Stora, T.; Lakey, J. H.; Vogel, H. *Angew. Chem., Int. Ed.* **1999**, *38*, 389–392.

(16) Johnson, S. J.; Bayerl, T. M.; McDermott, D. C.; Adam, G. W.; Rennie, A. R.; Thomas, R. K.; Sackmann, E. *Biophys. J.* **1991**, *59*, 289–294.

(17) Kühner, M.; Tampé, R.; Sackmann, E. *Biophys. J.* **1994**, *67*, 217–226.

(18) Wong, J. Y.; Park, C. K.; Steitz, M.; Israelachvili, J. N. *Biophys. J.* **1999**, *77*, 1458–1468.

(19) Heise, S.; Ernst, O. P.; Dienes, Z.; Hoffman, K. P.; Vogel, H. *Biochemistry* **1998**, *37*, 507–522.

(20) Wagner, M. L.; Tamm, L. K. *Biophys. J.* **2000**, *79*, 1400–1414.

to form a stable support for lipid bilayers. This problem can be overcome by covalently linking the unbranched PEG chain at one end to the hydrophilic support (e.g., quartz, oxidized silicon wafer) and the other end to some of the lipids in the supported membrane. The result of this design is a "tethered" polymer-supported lipid bilayer.²⁰ We found that several integral membrane proteins could be functionally reconstituted into tethered PEG-supported bilayers, where they exhibited a significant degree of lateral mobility.^{20,21} Therefore, these proteins were largely unconstrained by the hard inorganic substrate. Very recently, we measured the thickness of the polymer layer, that is, the distance between the solid support and the planar lipid bilayer, by fluorescence interference contrast microscopy. This cleft distance was 1.7 nm in the absence of the polymer but was increased to 3.9 nm in the presence of the covalently tethered PEG3400 polymer.²²

Attenuated total reflection Fourier transform infrared (ATR-FTIR) spectroscopy has become a powerful tool to probe secondary structures, orientations, lipid-protein interactions, and protein-protein interactions in supported membranes.²³ To our knowledge, PEG-supported bilayers have not yet been examined by ATR-FTIR spectroscopy. In the present work, we seek to characterize tethered PEG-supported lipid bilayers by ATR-FTIR spectroscopy. Specifically, we are interested to find out whether the polymer interferes in any way with ATR-FTIR measurements and whether the structure and order of the lipids in these bilayers are significantly affected by the polymer support.

A second aspect of this work is concerned with the structure and interactions of soluble *N*-ethylmaleimide-sensitive factor-attachment protein receptor (SNARE) fusion proteins as measured by ATR-FTIR spectroscopy. Neurons are electrically connected through chemical synapses. Neurotransmitters are released into the synaptic cleft from presynaptic vesicles that fuse with the presynaptic cell membrane of the firing neuron in a matter of milliseconds. Fusion of presynaptic vesicles with presynaptic target (cell) membranes is mediated by SNARE proteins.²⁴ There are two types of SNARE proteins, that is, v-SNAREs on the vesicles and t-SNAREs on the target membranes. According to the SNARE hypothesis, pairing of v- and t-SNAREs triggers membrane fusion.²⁴ Although the SNARE hypothesis has been refined from its original version several times and although the exact roles of v- and t-SNAREs in presynaptic membrane fusion are still debated, it is clear that v-t-SNARE interactions do take place at some time in the process of presynaptic membrane fusion. The v-SNARE consists of a single polypeptide chain called vesicle-associated membrane protein (VAMP), which has a relative molar mass of 12.7 kDa.²⁵ VAMP contains a single transmembrane anchor at its C-terminus. The t-SNARE consists of two polypeptide chains, namely, the integral membrane protein syntaxin ($M_r = 35$ kDa) and the lipid-anchored protein synaptosome-associated protein of 25 kDa (SNAP-25).²⁶ Syntaxin and SNAP-25 form a parallel three-helix

bundle. When VAMP binds to syntaxin/SNAP-25 it forms the so-called SNARE complex, which consists of a parallel four-helix bundle with the fourth helix contributed by VAMP.²⁷ Since the transmembrane (TM) domains are located at the C-termini of VAMP and syntaxin, they protrude from the same end, that is, the membrane proximal end of the four-helix bundle. In a construct in which the TM domain is deleted, the four-helix bundle of the SNARE complex protrudes 12–14 nm from the membrane surface.²²

In the present work, we have studied SNARE complex formation in supported membranes by ATR-FTIR spectroscopy and by total internal reflection fluorescence microscopy (TIRFM). We find that (i) t-SNAREs are stably incorporated into lipid bilayers, (ii) v-SNAREs are incorporated into lipid bilayers in a reversible fashion such that they can be extracted by an excess of pure or t-SNARE-containing lipid vesicles, and (iii) the secondary structure and lipid interactions are not profoundly changed by SNARE complex formation.

Experimental Procedures

Supported Bilayers. Supported bilayers were formed as previously described.^{20,28} Briefly, the substrates were cleaned as follows. Quartz slides ($40 \times 25 \times 1$ mm³; Quartz Scientific, Fairport Harbor, OH) to be used for TIRFM measurements were boiled in 10% Contrad 70 (Fisher Scientific), sonicated in hot detergent in a bath sonicator, and extensively rinsed with distilled water, followed by soaking in a concentrated H₂SO₄ and 30% H₂O₂ mixture at a volume ratio of 3:1 and extensive rinsing with distilled water and methanol. Germanium ATR plates ($50 \times 20 \times 1$ mm³ with 45° beveled edges; Spectral Systems, Irvington, NY) were cleaned by sonication for 2 h in 250 mM HCl in methanol and subsequent extensive rinsing with methanol. Both kinds of substrates were dried in an oven at 70 °C and, immediately before use, were plasma-cleaned in an argon plasma cleaner (Harrick Scientific, Ossining, NY) for 10 min.

Lipid monolayers consisting of 97 mol % 1-palmitoyl-2-oleoyl-*sn*-glycero-3-phosphocholine (POPC) (Avanti Polar Lipids, Alabaster, AL) and 3 mol % 1,2-dimyristoyl-*sn*-glycero-3-phosphoethanolamine-poly(ethylene glycol)3400-triethoxysilane (DPS) (20; custom-synthesized by Shearwater Polymers, Huntsville, AL) were spread from a 10 mM solution in chloroform at zero pressure at the air-water interface of a Langmuir-Blodgett (LB) trough (Nima 611, Coventry, U.K.). The subphase was 10 mM Tris-acetic acid buffer, pH 5.0, made from double-distilled water. The solvent was allowed to evaporate for 20 min before the monolayer was compressed at a rate of 30 cm²/min to a final surface pressure of 32 mN/m. The monolayer was kept at 32 mN/m for 15 min to reach equilibrium. Plasma-cleaned slides were quickly (200 mm/min) immersed through the monolayer and into the trough. Monolayers were transferred by withdrawing the slides from the subphase at a rate of 5 mm/min at a constant surface pressure of 32 mN/m. Monolayer transfer ratios very close to 100% were routinely achieved during withdrawal.

Large Unilamellar Vesicles. A certain amount of POPC was dissolved in chloroform, dried on the bottom of glass test tubes by a stream of nitrogen, desiccated under vacuum for 1 h, and hydrated by the addition of HEPES buffer (10 mM *N*-[2-hydroxyethyl]piperazine-*N'*-[2-ethanesulfonic acid] (HEPES), pH 7.4, containing 150 mM NaCl) to give the desired lipid concentration. The resulting lipid suspensions were vigorously vortexed, freeze-thawed five times, and extruded nine times through two polycarbonate membranes of 100 nm pore size, using a syringe-type extruder (Avestin, Ottawa, ON, Canada).

Fluorescent Labeling and Reconstitution of t-SNAREs and v-SNAREs into Phospholipid Vesicles. Expressed full-length syntaxin1A/SNAP-25 and VAMP2 were kind gifts of Dr. James Rothman (Memorial Sloan-Kettering Cancer Center, New York). These proteins were stored at -80 °C in small aliquots

(21) Wagner, M. L.; Tamm, L. K. *Biophys. J.* **2001**, *81*, 266–275.

(22) Kiessling, V.; Tamm, L. K. *Biophys. J.* **2003**, *84*, 408–418.

(23) Tamm, L. K.; Tatulian, S. A. *Q. Rev. Biophys.* **1997**, *30*, 365–429.

(24) Söllner, T. H.; Whiteheart, S. W.; Brunner, M.; Erdjument-Bromage, H.; Geromanos, S.; Tempst, P.; Rothman, J. E. *Nature* **1993**, *362*, 318–324.

(25) Südhof, T. C.; Baumert, M.; Perin, M. S.; Jahn, R. *Neuron* **1989**, *2*, 1475–1481.

(26) Bennett, M. K.; Calakos, N.; Scheller, R. H. *Science* **1992**, *257*, 255–259.

(27) Sutton, R. B.; Fasshauer, D.; Jahn, R.; Brünger, A. T. *Nature* **1998**, *395*, 347–353.

(28) Han, X.; Tamm, L. K. *J. Mol. Biol.* **2000**, *304*, 953–965.

in 25 mM HEPES/KOH (pH 7.4) containing 100 mM KCl, 10% glycerol, 2 mM 2-mercaptoethanol, 200 mM imidazol, and 1.0% β -octylglucoside (β -OG) (Sigma, St. Louis, MO). The proteins were thawed on ice as needed, stored at 4 °C, and used within 1 week. For fluorescence experiments, the proteins were fluorescently labeled by reacting with Alexa Fluor 488 succinimidyl ester (Molecular Probes, Eugene, OR) after adjusting the pH to 8.3 with 1 M sodium bicarbonate. The resulting Alexa 488/protein ratio was 3:1 (mol/mol) for syntaxin1A/SNAP-25 and 4:1 (mol/mol) for VAMP2 as determined by absorbance spectroscopy (a molar extinction coefficient of 71 000 at 494 nm was used for Alexa 488) and the Biorad protein assay²⁹ (Biorad, Hercules, CA). Alexa 488 labeled SNAREs were stored at 4 °C until used (not more than 1 week).

For reconstitution into lipid vesicles, POPC was taken from a chloroform stock solution, dried under N₂, and placed under vacuum for 30 min. The dried lipid films were fully solubilized with a volume of 1.0% β -OG in reconstitution buffer (RB; 25 mM HEPES/KOH, 100 mM KCl, pH 7.4) followed by the addition of a volume of the protein in protein buffer to give a final volume of 0.5 L and the desired protein/lipid ratio. The mixture was equilibrated at room temperature for 1 h followed by addition of 1.0 L of RB to bring the β -OG concentration below the critical micellar concentration. The mixture was dialyzed for 48 h against 1.0 L of RB at 4 °C with two changes of buffer after 4 and 24 h, respectively. The lipid/protein ratio was routinely determined by the Biorad protein assay and a modified Ames phosphate assay to estimate lipid concentration.³⁰

Reconstitution of t-SNAREs and v-SNAREs into Polymer-Supported Bilayers. Syntaxin1A/SNAP-25 and VAMP2 were reconstituted into polymer-supported bilayers by fusion of syntaxin1A/SNAP-25 and VAMP2 vesicles to a polymer-supported monolayer. A dry DPS-supported monolayer (POPC/DPS, 97:3) was transferred onto the appropriate substrate by the Langmuir–Blodgett technique as described above. The supported monolayers were assembled in perfusable ATR or TIRFM measuring cells. Supported bilayers were formed by the addition of 0.9 mL (ATR) or 1.1 mL (TIRFM) of protein-containing vesicles (100 μ M lipid). Vesicles are known to spread on supported monolayers and form supported bilayers under these conditions.³¹ After 2 h of equilibration at room temperature, the TIRFM measuring cell was flushed with 10 mL of RB adjusted to pH 5.0, followed by a 20 min equilibration before returning the pH to 7.4 by flushing with 10 mL of RB. Excess vesicles are removed and the homogeneity of the bilayer is improved in this step. Because the first (LB-deposited) monolayer contains only lipids and no protein, the lipid/protein ratio of the subsequently formed protein containing bilayer is approximately twice the lipid/protein ratio of the reconstituted vesicles from which it has been derived. The ATR measuring cell was flushed with 3.5 mL of D₂O HEPES buffer (10 mM HEPES/NaOH, 150 mM NaCl, pH 7.4), which was also used in the ATR-FTIR background scans.

SNARE Complex Formation in Planar Polymer-Supported Lipid Bilayers. After formation of DPS-supported syntaxin1A/SNAP-25 bilayers, 0.9 or 1.1 mL of diluted VAMP2 vesicles (100 μ M lipid) were injected into the ATR or TIRFM measuring cells, respectively. After 2 h of equilibration at room temperature, excess unbound VAMP2 vesicles were flushed out with 3.5 mL of D₂O HEPES buffer in the ATR experiments or with 10 mL of RB in the TIRFM experiments. For the case of the fluorescent VAMP2, the kinetics of binding was monitored by TIRFM.

Circular Dichroism Spectroscopy. Circular dichroism spectra were recorded on an AVIV model 215 spectropolarimeter (AVIV, Lakewood, NJ). Syntaxin1A/SNAP-25 and VAMP2 vesicles were diluted in RB buffer to appropriate concentrations (2.5–25 μ M protein). Spectra were measured in a 0.5 mm path length cuvette at room temperature. Six scans recorded at a rate of 10 nm/min between 200 and 250 nm and a spectral resolution of 0.5 nm were averaged for each spectrum. The corresponding reference spectra of pure POPC vesicles in RB buffer were

subtracted in each case. Mean residue molar ellipticities, $[\theta]$, were calculated by

$$[\theta] = \frac{\theta}{n \times \text{concn} \times \text{path length} \times 10} \text{ [deg cm}^2 \text{ dmol}^{-1}] \quad (1)$$

where θ is the ellipticity in millidegrees, n is the number of amino acid residues in the protein, and concn is the molar concentration of the protein. The path length is measured in millimeters.

ATR-FTIR Spectroscopy. ATR-FTIR measurements were carried out on a Bruker VECTOR 22 (Bruker Instruments, Billerica, MA) Fourier transform infrared spectrometer equipped with a 25 reflection variable angle ATR accessory (Specac Inc., Smyrna, GA) and a motorized wire grid polarizer (Bruker Instruments). After the instrument and sample compartment were purged with dry air for 2 h to remove H₂O vapor, 200 scans were collected at parallel and perpendicular polarization with a nominal resolution of 4 cm⁻¹. The corresponding polarized ATR spectra of the respective D₂O buffers were used as references. Spectra were fast Fourier transformed with a Blackman-Harris 3-term apodization function and 2N zero-filling. Lipid order parameters, defined as

$$S_L = \frac{1}{2}(3 \cos^2 \theta - 1) \quad (2)$$

where the angular brackets denote an average of all angles θ between the molecular director and the membrane normal in the sample, were calculated as described²³ using the thin film approximation ($E_x^2 = 1.9691$, $E_y^2 = 2.2486$, $E_z^2 = 1.8917$):

$$S_L = -2 \frac{E_x^2 - R^{\text{ATR}} E_y^2 + E_z^2}{E_x^2 - R^{\text{ATR}} E_y^2 - 2E_z^2} \quad (3)$$

Total Internal Reflection Fluorescence Microscopy and Fluorescence Recovery after Photobleaching. The laser fluorescence microscope built around a Zeiss Axiovert 35 (Carl Zeiss, Thornwood, NY) that was used for imaging supported membranes and for TIRFM and fluorescence recovery after photobleaching (FRAP) experiments has been described in detail elsewhere.^{31,32} Epifluorescence micrographs were taken using a 40 \times water-immersion objective and an EG&G 512 \times 512 cooled CCD camera (PARC, Princeton, NJ). For TIRFM, the beam of an argon ion laser (Innova 300-8, Coherent, Palo Alto, CA) was set at 488 nm and directly focused through a trapezoid quartz prism to the lower surface of a quartz slide with the supported membrane, which forms the ceiling of the TIRFM measuring cell. The beam was totally internally reflected at the quartz–buffer interface at an incident angle of 72° from the normal (the critical angle is 65°). An elliptical area, approximately 250 \times 65 μ m², was illuminated. Fluorescence resulting from excitation by the evanescent wave, which penetrates about \sim 90 nm (1/e) into the adjacent buffer phase, was collected with a photomultiplier tube through the 40 \times water-immersion objective of the microscope. FRAP experiments were carried out on the same samples and on the same microscope by bleaching a pattern of parallel stripes, formed by imaging a Ronchi ruling into the image plane, and recording the integrated fluorescence recovery of an approximately 100 μ m² area as a function of time. Fluorescence recovery curves were fit to the equation

$$F(t) = F_\infty + (F_0 - F_\infty) \exp(-D_L a^2 t) \quad (4)$$

where $a = 2\pi/p$, D_L is the lateral diffusion coefficient, p is the stripe period, and F_0 and F_∞ are the fluorescence intensities immediately after and a very long time after the bleach pulse, respectively. The mobile fraction in percent is calculated by

$$\text{mobile fraction} = [(F_\infty - F_0)/(F_{\text{pre}} - F_0)] \times 200 \quad (5)$$

where F_{pre} is the fluorescence intensity before the bleach pulse.

(29) Bradford, M. *Anal. Biochem.* **1976**, *72*, 248–254.
 (30) Ames, B. N. *Methods Enzymol.* **1966**, *8*, 115–118.
 (31) Kalb, E.; Frey, S.; Tamm, L. K. *Biochim. Biophys. Acta* **1992**, *1103*, 307–316.

(32) Kalb, E.; Engel, J.; Tamm, L. K. *Biochemistry* **1990**, *29*, 1607–1613.

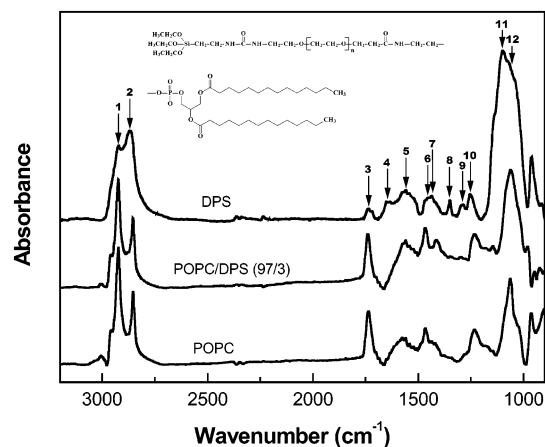


Figure 1. ATR-FTIR spectra of dry monolayers of DPS, POPC/DPS (97/3), and POPC on a germanium ATR plate. The assignments of the numbered peaks are listed in Table 1. The chemical structure of DPS is shown at the top. The average number of glycol units is $n = 77$.

Results

FTIR Spectra of the PEG-Lipid DPS. To interpret ATR-FTIR spectra of proteins that are bound to or incorporated in tethered polymer-supported planar lipid bilayers, we first characterized the spectroscopic features of the polymer-lipid DPS. An overview ATR-FTIR spectrum of a single monolayer of pure DPS is shown in Figure 1. For comparison, ATR-FTIR spectra of a pure POPC monolayer and a monolayer of a mixture of 97 mol % POPC and 3 mol % DPS are also shown in Figure 1. These spectra were all recorded with dry Langmuir-Blodgett deposited monolayers. Assignments that are based on these spectra and published infrared absorption frequencies of lipids,²³ PEG,³³ and silanes³⁴ are listed in Table 1. The most prominent differences between DPS and POPC are (i) a much broader and blue-shifted CH₂ symmetric stretching vibration at ~ 2870 cm⁻¹ for DPS, which probably reflects the heterogeneous environments of the PEG methylene groups, (ii) decreased C=O stretching and CH₂ scissoring bands in DPS, and (iii) much increased and broader CH₂-O-CH₂ stretching vibrations at 1130–1020 cm⁻¹ for DPS that are superimposed on the O-P-O, CO-O-CH₂, and CH₂-O-P-O-CH₂ stretching vibrations of the phospholipids headgroups at 1085, 1070, and 1060 cm⁻¹, respectively. A few new bands appear in the fingerprint region of DPS between 1600 and 1200 cm⁻¹ that are not present in POPC. They are tentatively assigned to the PEG CH₂ scissoring band at 1450 cm⁻¹, the PEG antisymmetric CH₂-O-CH₂ stretch at 1348 cm⁻¹, and the PEG symmetric CH₂-O-CH₂ stretch at 1288 cm⁻¹. Additionally, a weak amide I band at 1653 cm⁻¹ is seen in the DPS spectrum that arises from the two amide linkages in DPS. As expected, the mixed monolayer of POPC and DPS is dominated by the POPC spectrum but still contains some weak features of DPS. Importantly, it shows that the regions that we are mostly interested in for examining lipid-protein interactions, namely, 3000–2800, ~ 1730 , and ~ 1650 cm⁻¹, are not significantly affected by DPS at the chosen concentration of 3 mol %.

FTIR Spectroscopy of DPS-Supported Lipid Bilayers. We examined whether the polymer cushion that separates supported lipid bilayers from the solid support

Table 1. Observed Infrared Absorption Frequencies of DPS and POPC Monolayers and Corresponding Assignments

| peak number ^a | wavenumber (cm ⁻¹) | assignment |
|--------------------------|--------------------------------|---|
| DPS Monolayer | | |
| 1 | 2923 | CH ₂ antisymmetric stretch |
| 2 | 2869 | CH ₂ symmetric stretch |
| 3 | 1735 | C=O stretch |
| 4 | 1653 | amide I stretch |
| 5 | 1576 | |
| 6 | 1468 | aliphatic CH ₂ scissoring |
| 7 | 1450 | glycol CH ₂ scissoring |
| 8 | 1348 | glycol (OCH ₂ -CH ₂) chain antisymmetric stretch |
| 9 | 1288 | glycol (OCH ₂ -CH ₂) chain symmetric stretch |
| 10 | 1252 | PO ₂ ⁻ antisymmetric stretch |
| 11 | 1130–1020 | various glycol (CH ₂ -O-CH ₂) chain stretches and Si-O-CH ₂ stretches |
| POPC Monolayer | | |
| 1 | 2923 | CH ₂ antisymmetric stretch |
| 2 | 2853 | CH ₂ symmetric stretch |
| 3 | 1735 | C=O stretch |
| 5 | 1576 | |
| 6 | 1463 | CH ₂ scissoring |
| 10 | 1231 | PO ₂ ⁻ antisymmetric stretch |
| 12 | 1090–1030 | PO ₂ ⁻ symmetric stretch and CO-O-CH ₂ symmetric stretch |

^a Refers to peak numbers in Figure 1.

had any effect on the bilayer structure that could be detected by ATR-FTIR spectroscopy. We previously determined by fluorescence microscopy and lateral diffusion experiments that a concentration of 3 mol % of DPS in the substrate-exposed inner monolayer was optimal for supported bilayer formation.²⁰ Therefore, we compare in Figure 2 polarized ATR-FTIR spectra of supported lipid bilayers with and without the 3 mol % polymer cushion. In contrast to the monolayer spectra of Figure 1, these (and all following) spectra were obtained in an aqueous (D₂O) buffer solution. The bilayer spectra are essentially unaffected by the presence of the polymer. The positions of the symmetric and antisymmetric methylene stretching vibrations are at 2852 and 2924 cm⁻¹, respectively, as expected for lipid bilayers in the liquid-crystalline phase. From the dichroic ratios of these bands (Table 2), we calculate acyl chain order parameters of 0.01–0.04 in the absence or presence of the polymer. These values are small and indicate disorder of the lipid acyl chains. The disorder of the unsaturated acyl chains observed here is larger than what we typically observe for lipid bilayers with saturated acyl chains in the liquid-crystalline phase.²³

The v-SNARE VAMP2 in DPS-Supported Lipid Bilayers. Figure 3 shows polarized ATR-FTIR spectra of VAMP2 reconstituted into DPS-supported lipid bilayers in the lipid methylene region (panel A) and the lipid carbonyl and protein amide I region (panel B). Numerical values of the observed peak frequencies and dichroic ratios are listed in Table 2. A comparison of the corresponding numbers in Table 2 shows that the lipids are not perturbed to any significant degree by the presence of the VAMP2. The maximum of the amide I band is at 1649 cm⁻¹ with a broad shoulder reaching to below 1600 cm⁻¹. The peak position would be consistent with α -helical or random coil secondary structure, but the shoulder indicates more random and perhaps some extended β -strand secondary structures.²³ To confirm the secondary structure of VAMP2 in lipid vesicles, we recorded circular dichroism (CD) spectra of these samples (Figure 4). The CD spectra of VAMP2 do not show much of any regular secondary

(33) Pouchert, C. J. *The Aldrich Library of FTIR Spectra*, 2nd ed.; Aldrich Chemical Co.: Milwaukee, WI, 1985; pp 1168–1171.

(34) Socrates, G. *Infrared Characteristic Group Frequencies*, 2nd ed.; John Wiley & Sons: New York, 1994.

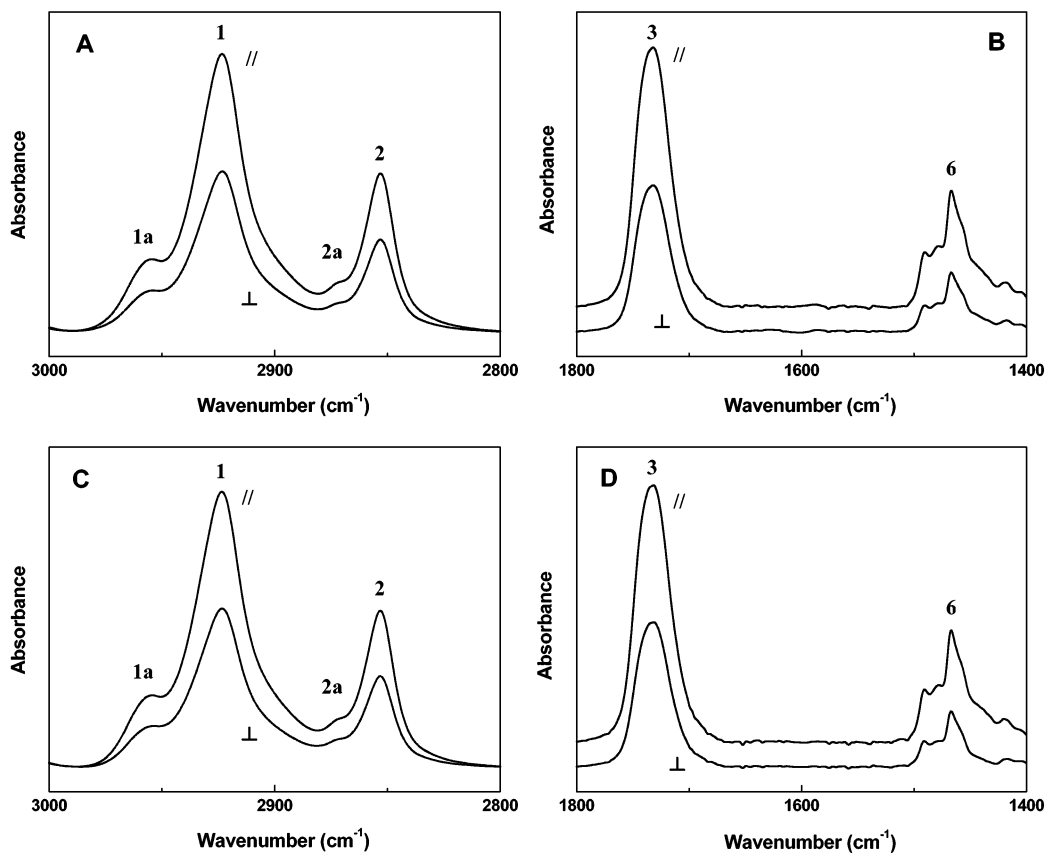


Figure 2. Polarized ATR-FTIR spectra of supported POPC in the methylene stretching (A,C) and the carbonyl and methylene scissoring (B,D) regions without (A,B) and with a 3 mol % DPS cushion (C,D). The spectra of bilayers on germanium ATR plates were collected in D₂O HEPES buffer. Peak numbers correspond to the assignments in Table 1, and dichroic ratios are listed in Table 2. Peaks 1a and 2a correspond to the antisymmetric and symmetric terminal methyl stretch vibrations, respectively. Supported bilayers were formed by fusion of vesicles prepared in D₂O buffer to a supported monolayer containing 3 mol % DPS.

Table 2. Frequencies and Dichroic Ratios of Major Lipid and Protein Infrared Absorption Bands of DPS-Supported Bilayers with and without Reconstituted SNARE Proteins

| | wavenumber (cm ⁻¹) | dichroic ratio ^a (A ₀ /A ₉₀) | assignment |
|---|-----------------------------------|---|---------------------------------------|
| quartz-supported POPC bilayer | 2924 | 1.70 ± 0.04 | CH ₂ antisymmetric stretch |
| | 2852 | 1.68 ± 0.05 | CH ₂ symmetric stretch |
| | 1732 | 1.90 ± 0.06 | C=O stretch |
| DPS (3 mol %)-supported POPC bilayer | 2924 | 1.70 ± 0.06 | CH ₂ antisymmetric stretch |
| | 2853 | 1.67 ± 0.07 | CH ₂ symmetric stretch |
| | 1734 | 1.98 ± 0.04 | C=O stretch |
| DPS-supported bilayer with reconstituted VAMP2 | 2924 | 1.81 ± 0.04 | CH ₂ antisymmetric stretch |
| | 2853 | 1.78 ± 0.04 | CH ₂ symmetric stretch |
| | 1732 | 1.85 ± 0.05 | C=O stretch |
| | 1649 | 2.94 | amide I |
| DPS-supported bilayer with reconstituted syntaxin1A/SNAP-25 | 2924 | 1.74 ± 0.03 | CH ₂ antisymmetric stretch |
| | 2853 | 1.72 ± 0.04 | CH ₂ symmetric stretch |
| | 1734 | 1.83 ± 0.04 | C=O stretch |
| | 1649 | 1.75 ± 0.18 | amide I |
| DPS-supported bilayer with reconstituted syntaxin1A/SNAP-25 and after binding of VAMP2 vesicles | 2924 | 1.77 ± 0.03 | CH ₂ antisymmetric stretch |
| | 2853 | 1.75 ± 0.03 | CH ₂ symmetric stretch |
| | 1734 | 1.81 ± 0.03 | C=O stretch |
| | 1647 | 2.27 ± 0.43 | amide I |
| DPS-supported bilayer with reconstituted syntaxin1A/SNAP-25 and after incubation with POPC vesicles | 2924 | 1.78 ± 0.04 | CH ₂ antisymmetric stretch |
| | 2853 | 1.75 ± 0.04 | CH ₂ symmetric stretch |
| | 1732 | 1.84 ± 0.04 | C=O stretch |
| | 1649 | 1.97 ± 0.05 | amide I |

^a Averages from 2–3 experiments.

structure and are characteristic of a protein in a mostly random coil conformation. The CD spectra in vesicles and FTIR spectra in supported bilayers are therefore totally consistent with each other, indicating mostly random coils of membrane-bound VAMP2. The high dichroic ratio of 2.94 of the amide I band suggests that the disordered polypeptide chain of VAMP2 might be aligned in some

way along the membrane surface rather than extending completely randomly into the aqueous environment.

Interestingly, membrane-bound VAMP2 can exchange between different lipid bilayers. This is shown in panels C and D of Figure 3. When the measuring cell was flushed with an excess of pure POPC vesicles, VAMP2 was extracted from the supported lipid bilayer as seen by the

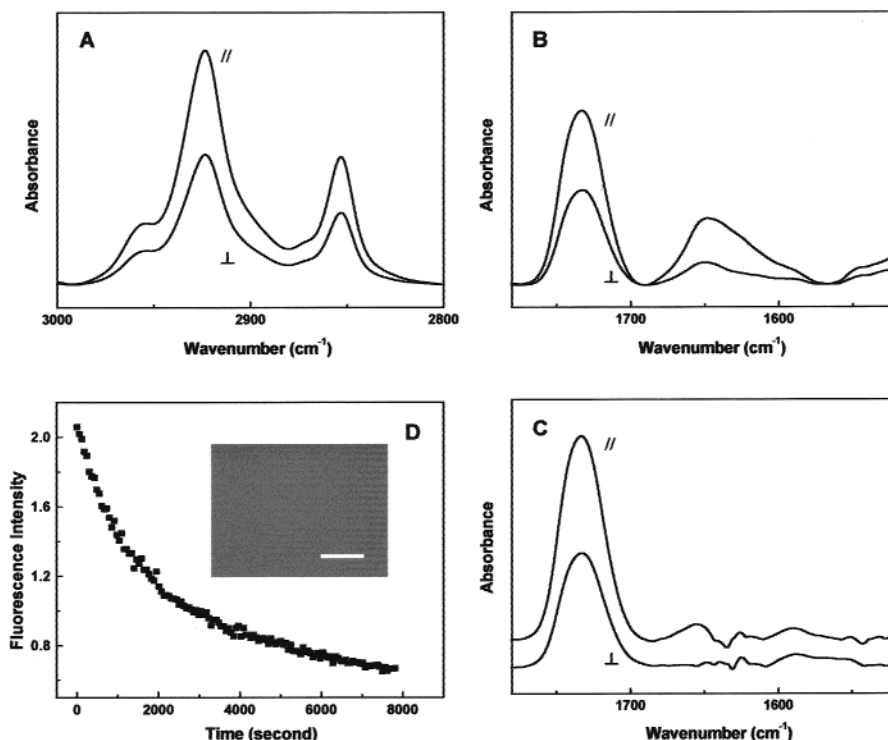


Figure 3. Polarized ATR-FTIR spectra and TIRFM measurements of reconstituted VAMP2 in a DPS-supported POPC bilayer. Polarized ATR-FTIR spectra are shown in the methylene stretching region (A) and the lipid ester carbonyl and protein amide I and II regions (B,C). The lipid/protein ratio in the supported bilayers was 800:1. (C) shows the spectra of the same bilayer as (B), but after incubation with 100 μM POPC vesicles. (D) TIRFM experiment showing the kinetics of the extraction of VAMP2 from a reconstituted VAMP2-containing DPS-supported bilayer after incubation with 100 μM POPC vesicles. The bilayer contained Alexa 488 labeled VAMP2 at a lipid/protein ratio of 800:1 at the beginning of the experiment. The inset shows a TIRF micrograph of the distribution of VAMP2 in the DPS-supported lipid bilayer before the beginning of the extraction of VAMP2. The bar is 50 μm .

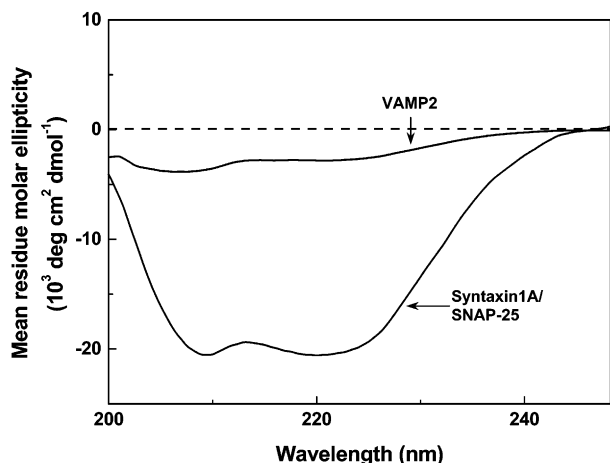


Figure 4. CD spectra of syntaxin1A/SNAP-25 and VAMP2 reconstituted in small unilamellar vesicles of POPC in HEPES buffer at pH 7.4. The syntaxin1A/SNAP-25 concentration was 2.5×10^{-6} M, the VAMP2 concentration was 2.5×10^{-5} M, and the lipid concentration was 1×10^{-4} M in both preparations.

disappearance of the amide I band in panel C. When the cell was flushed with pure buffer, VAMP2 remained stably attached to the supported lipid bilayer and the spectra were virtually identical to those shown in panel B (data not shown). This strongly suggests that VAMP2 can readily transfer between two lipid bilayers. To measure the kinetics of this transfer, we performed a TIRFM experiment with Alexa 488 labeled VAMP2 (panel D). A fluorescence micrograph of the polymer-supported membrane with Alexa 488 labeled VAMP2 shows a uniformly stained surface and, therefore, indicates a homogeneous

distribution of VAMP2 in the membrane (inset of panel D). The fluorescence disappeared gradually over a time period of about 2 h after the supported membrane was incubated with POPC vesicles (panel D). No decrease in fluorescence intensity was observed when the same membranes were treated with buffer instead of POPC vesicles (data not shown).

The t-SNARE Syntaxin1A/SNAP-25 in DPS-Supported Lipid Bilayers. Figure 5 shows polarized ATR-FTIR spectra of syntaxin1A/SNAP-25 reconstituted into DPS-supported lipid bilayers in the lipid methylene region (panel A) and the lipid carbonyl and protein amide I region (panel B). Numerical values of the observed peak frequencies and dichroic ratios are listed in Table 2. Similar to the results observed for the case of VAMP2, the lipids are not significantly perturbed by the presence of syntaxin1A/SNAP-25. However, the amide I band of the t-SNARE centered at 1649 cm^{-1} was much more symmetric than that of VAMP2 (panel B). This feature is indicative of well-ordered α -helices.²³ The dichroic ratio of 1.75 yields an order parameter close to zero, which indicates either a random distribution of the helices or an orientation close to the "magic angle" of 54.7° from the membrane normal. Unfortunately, it is not possible to distinguish between these two possibilities or their combinations based on these polarized FTIR measurements alone. In contrast to VAMP2, the t-SNARE cannot be extracted from the planar membranes by POPC vesicles. The amide I band remains after incubation with POPC vesicles (panel C), and the fluorescence of Alexa 488 labeled syntaxin1A/SNAP-25 does not decrease in the TIRFM experiment. Also in contrast to VAMP2, the t-SNAREs appear as clusters in

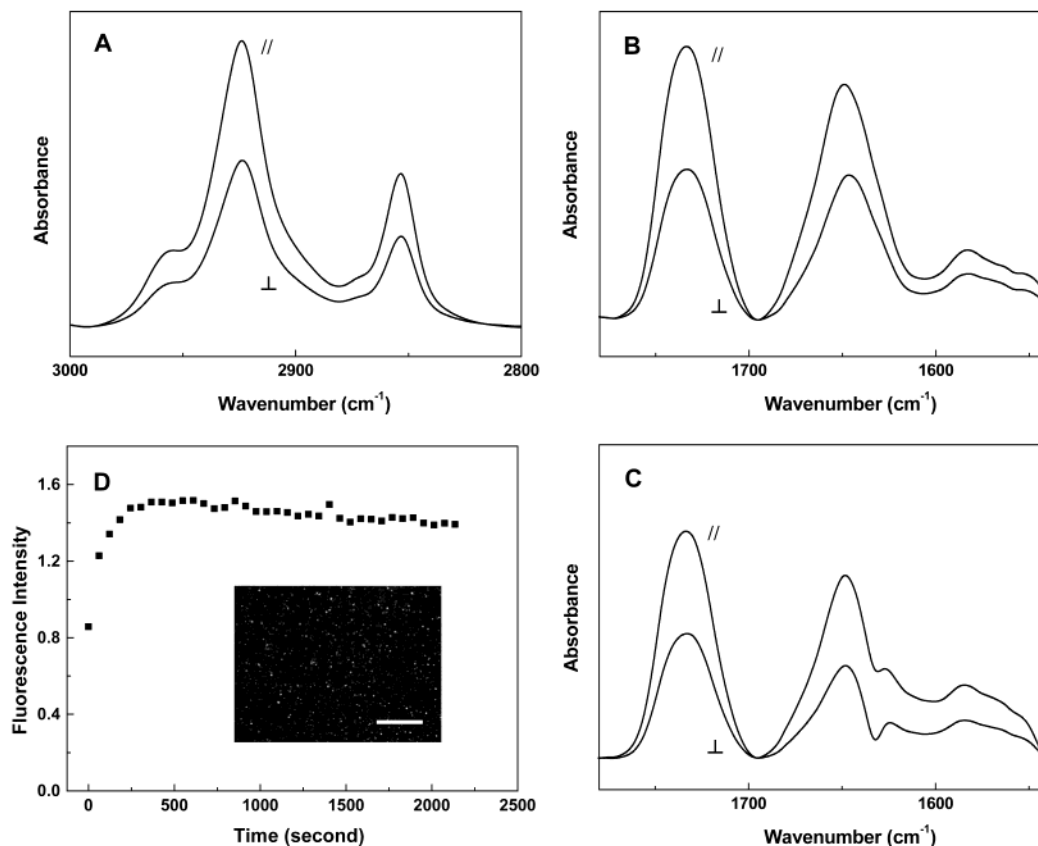


Figure 5. Polarized ATR-FTIR spectra and TIRFM measurements of reconstituted syntaxin1A/SNAP-25 in a DPS-supported POPC bilayer. Polarized ATR-FTIR spectra are shown in the methylene stretching region (A) and the lipid ester carbonyl and protein amide I and II regions (B,C). The lipid/protein ratio in the supported bilayers was 800:1. (C) shows the spectra of the same bilayer as (B), but after incubation with 100 μM POPC vesicles. (D) TIRFM experiment showing the fluorescence intensity increase after incubation of the DPS-supported monolayer with POPC/syntaxin1A/SNAP-25 vesicles (lipid/protein 1600:1) to form a DPS-supported bilayer. The syntaxin1A/SNAP-25 was labeled with Alexa 488. The inset shows a TIRF micrograph of the distribution of syntaxin1A/SNAP-25 in the DPS-supported lipid bilayer. The bar is 50 μm .

the membrane as shown in the micrograph in the inset of panel D.

Interaction of v-SNAREs and t-SNAREs in DPS-Supported Lipid Bilayers. We wanted to know whether binding of reconstituted VAMP2 in vesicles to reconstituted syntaxin1A/SNAP-25 (t-SNARE) in DPS-supported bilayers, that is, formation of the four-helix bundle SNARE complex, would change the secondary structure and/or orientation of these proteins relative to the plane of the supported membrane. We also asked in these experiments whether the formation of SNARE complexes in supported bilayers affected the structure of the lipid bilayer in a way that would lead to changes in any of the lipid-associated ATR-FTIR absorption bands. Figure 6 shows polarized ATR-FTIR spectra of SNARE complexes formed in supported bilayers in the lipid methylene (panel A) and the lipid carbonyl and protein amide I regions (panel B). Numerical values of the observed peak frequencies and dichroic ratios are listed in Table 2. Figure 6C shows a TIRFM experiment demonstrating the binding of Alexa 488 labeled VAMP2 in vesicles to reconstituted syntaxin1A/SNAP-25 in a DPS-supported bilayer. The inset demonstrates that VAMP2 binds to the nonuniformly distributed t-SNAREs that were also seen in the absence of bound VAMP2 vesicles (cf. Figure 5D). It is apparent from the ATR-FTIR data that binding of VAMP2 had only a minor effect on the structure of the syntaxin1A/SNAP-25, which included a shift of the amide I peak frequency from 1649 to 1647 cm^{-1} and a possible increase of the amide I dichroic ratio from around 1.8 to around 2.2. The

lipid signals were not significantly affected by binding of the VAMP2 vesicles.

Discussion

The two major goals of this work were to examine the suitability of poly(ethylene glycol)-supported membranes for studies of lipid structure and lipid-protein interactions by ATR-FTIR spectroscopy and, as a first application, to investigate SNARE protein-protein and protein-lipid interactions in DPS-supported lipid bilayers by ATR-FTIR spectroscopy. These two aspects of the work will be discussed separately in the following sections.

ATR-FTIR Spectroscopy of DPS-Supported Membranes. The work presented here demonstrates that the DPS-supported model membrane system is adequate for ATR-FTIR spectroscopic studies of lipids and membrane proteins in physiologically relevant environments. It is shown that the infrared absorption bands of DPS at a concentration of 3 mol % in the inner, substrate-exposed monolayer do not significantly interfere with the absorption bands of the proteins and lipids that are commonly used to study secondary structures of membrane proteins and their interactions with membrane lipids. Since DPS is included only in the inner monolayer, the overall concentration of DPS in the bilayer is only 1.5 mol %. The most intense absorption bands of DPS occur at ~ 2870 cm^{-1} and a very broad spectral feature in the 1130–1020 cm^{-1} region. These bands can be assigned, respectively, to the aliphatic and glycol methylene stretching vibrations and a collection of highly overlapped bands corresponding

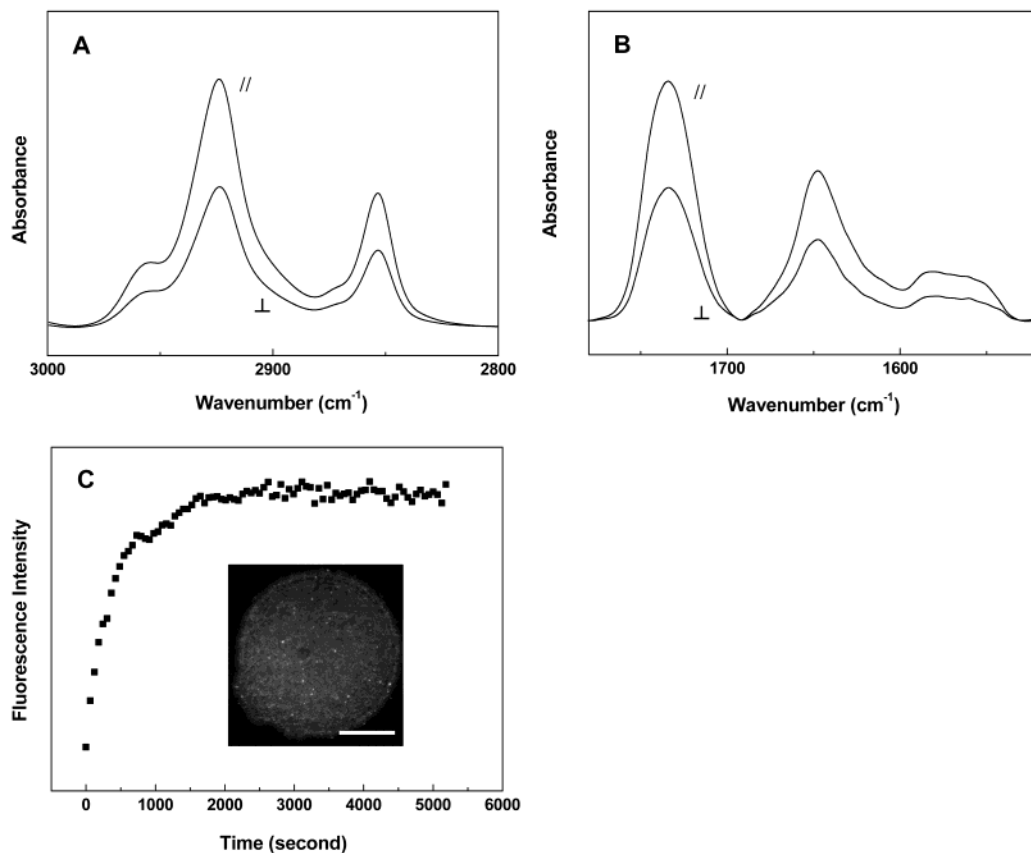


Figure 6. Polarized ATR-FTIR spectra of reconstituted syntaxin1A/SNAP-25 in a DPS-supported POPC bilayer (lipid/protein ratio, 800:1) in the methylene stretching region (A) and the lipid ester carbonyl and protein amide I and II regions (B) after 1.5 h of incubation with VAMP2 vesicles. (C) TIRFM experiment showing the binding kinetics of Alexa 488 labeled VAMP2 vesicles to a reconstituted syntaxin1A/SNAP-25-containing DPS-supported bilayer. The DPS-supported bilayer contained unlabeled syntaxin1A/SNAP-25 at a lipid/protein ratio of 400:1. The lipid/protein ratio of the VAMP2 vesicles was 200:1 in the TIRFM and 400:1 in the ATR-FTIR experiments. The inset shows a TIRFM micrograph of the distribution of Alexa 488 labeled VAMP2 bound to syntaxin1A/SNAP-25 in the DPS-supported lipid bilayer. The bar is 50 μm .

to various C–O stretching modes of the PEG units. Some Si–O stretching vibrations also absorb in the 1100–1000 cm^{-1} region. Even the subcomponents of these highly overlapped bands are rather broad because of the disordered nature of the ethylene glycol units in hydrated and dried PEG. The band at $\sim 2870 \text{ cm}^{-1}$ overlaps with the symmetric and antisymmetric lipid methylene stretching vibrations of DPS itself and of admixed lipids. However, since the aliphatic lipid methylene stretching vibrations are quite narrow and intense, they completely dominate the signal in this region when measured in a 3 mol % DPS-supported lipid bilayer. Therefore, it is possible to obtain accurate measurements of the lipid methylene stretching vibrations in DPS-supported membranes. This is not true for the spectral region around 1100 cm^{-1} , which in DPS-supported bilayers is greatly influenced by the PEG and possibly some Si–O stretching vibrations. Therefore, measurements of lipid phosphate and CO–O–CH₂ stretching vibrations, which also absorb in this spectral region, cannot be analyzed in the DPS-supported bilayer system. A few isolated DPS absorption bands may be analyzed in mixed POPC/DPS (97:3) monolayers. They are the PEG-associated bands at ~ 1348 and $\sim 1288 \text{ cm}^{-1}$. The antisymmetric phosphate stretching band at 1250–1230 cm^{-1} is common to both POPC and DPS. However, these vibrations are not easily observed in supported bilayers in D₂O buffers because they overlap with the strong and broad D₂O bending vibration, which is centered around 1210 cm^{-1} . The methylene scissoring bands of the lipid fatty acyl chains at 1460–1470 cm^{-1} are partially

obscured by the broader methylene scissoring bands of PEG in the 1460–1420 cm^{-1} spectral region.

The data of Figure 2 show that the polymer support did not significantly affect the bilayer structure as measured by polarized ATR-FTIR. The frequencies of the methylene stretching vibrations did not change when the polymer was intercalated between the bilayer and the support. These frequencies are known to depend on the phase state of the lipids. For example, lipids in the gel phase exhibit symmetric and antisymmetric stretching vibrations that are 4–6 cm^{-1} lower than those in the liquid-crystalline phase and 4–6 cm^{-1} lower than those reported here.³⁵ Therefore, the fatty acyl chains of the lipids in the polymer-supported lipid bilayers are ordered to the same degree as they are in unsupported bilayers in the liquid-crystalline phase. This notion is supported by the observation of very similar dichroic ratios and lipid acyl chain order parameters in lipid bilayers that are directly supported on germanium and in lipid bilayers that are supported on the PEG cushion.

The lipid ester carbonyl band at 1735 cm^{-1} is also not significantly affected by the presence of the PEG cushion under the bilayer. It has been shown that this band actually consists of two overlapped component bands at ~ 1742 and 1728 cm^{-1} that are due to dehydrated and hydrated carbonyl groups, respectively.³⁶ Therefore, this band is sensitive to hydration interactions in the polar

(35) Mendelsohn, R.; Mantsch, H. H. In *Progress in Protein–Lipid Interactions 2*; Watts, A., DePont, J. J. H. M., Eds.; Elsevier Science Publishers: Amsterdam, 1986; pp 103–146.

headgroup region of the lipids. Apparently, the hydration conditions in the polymer-supported bilayers are not dramatically altered compared to directly supported or unsupported lipid bilayers. If they were, a change in the position, width, or dichroic ratio of this band would have been observed.

The v-SNARE VAMP2 is unstructured in membranes and can exchange between membranes. Both CD and FTIR spectra of VAMP2 indicate that this integral membrane protein does not adopt much regular secondary structure in membranes. Previous CD and NMR studies of the soluble portion of VAMP2 (also referred to as synaptobrevin2; residues 1–96) indicate that this protein is unstructured in solution.^{37,38} Our studies with the full-length VAMP2 (116 residues) in lipid bilayer membranes confirm these earlier results. It is possible that the very small amount of residual secondary structure that is seen in our CD spectra (Figure 4) corresponds to the transmembrane domain (residues 97–116) of VAMP2. Neither this domain nor the presence of the membrane appears to induce additional secondary structure in the soluble portion of VAMP2.

A surprising new finding of this work is that VAMP2 can be extracted from membranes by the addition of pure lipid vesicles. Since the protein is not extracted by the addition of buffer, it must be transferred from one lipid membrane (the planar supported membrane) to another membrane (the vesicles). Most likely, this happens by a direct collision of these membranes. This unexpected result sheds some doubt on whether VAMP2 is truly a bona fide type I integral membrane protein with a regular helical transmembrane anchor domain at its C-terminus. Interestingly, peptides corresponding to the TM domain of VAMP2 exhibited significant amounts of β -structure in lipid bilayers but were more helical in reverse micelles.³⁹ This result suggested that VAMP2 may possess a conformationally flexible TM domain. Moreover, fusion of liposomes correlated with the disappearance of α -helical secondary structure in a series of mutations in peptide models of this region, suggesting that this conformational flexibility may be functionally important. Conformational flexibility has also been observed and shown to be of functional importance for several viral fusion peptides.⁴⁰ Therefore, it is tempting to speculate that the TM domain of VAMP2 is not a normal TM domain but actually functions as a fusion peptide capable of reversibly inserting into different lipid membranes in the course of a round of membrane fusion.

(36) Blume, A.; Hübner, W.; Messner, G. *Biochemistry* **1988**, *27*, 8239–8249.

(37) Fasshauer, D.; Eliason, W. K.; Brünger, A. T.; Jahn, R. *Biochemistry* **1998**, *37*, 10354–10362.

(38) Hazzard, J.; Südhof, T. C.; Rizo, J. *J. Biomol. NMR* **1999**, *14*, 203–207.

(39) Langosch, D.; Crane, J. M.; Brosig, B.; Tamm, L. K.; Reed, J. *J. Mol. Biol.* **2001**, *311*, 709–721.

(40) Tamm, L. K.; Han, X. *Biosci. Rep.* **2000**, *20*, 501–518.

The t-SNARE syntaxin1A/SNAP-25 is α -helical in membranes and does not significantly change its secondary structure upon binding of the v-SNARE VAMP2. It is not surprising that syntaxin1A/SNAP-25 forms a stable helical structure by itself. This has been shown before for the soluble portion of this protein in which the TM domain was deleted.^{37,41,42} It has been suggested that syntaxin1A exists in a closed and in an open conformation.⁴¹ In the closed conformation, the SNARE motif of syntaxin1A is dissociated from the SNARE motif of SNAP-25 but instead interacts with a shorter three-helix bundle of the N-terminal regulatory domain of syntaxin1A. In the open conformation, which is the conformation that binds VAMP2, a three-helix bundle is formed between the SNARE motifs of syntaxin1A and SNAP-25. Since both forms are highly helical, it is not possible to distinguish with the employed methods which form prevails under the various conditions of our studies. If the closed form is the predominant form in the reconstituted syntaxin1A/SNAP-25 supported bilayers, it must first open in order to bind VAMP2. Since we had to use quite large concentrations of VAMP2 vesicles to observe significant binding to the t-SNARE bilayers, we think that the closed conformation is more abundant in the supported membranes than the open conformation. Irrespective of the exact mechanism and order of SNARE protein binding in this new reconstituted model membrane system, it is clear that SNARE complex formation does not lead to a measurable increase in α -helical secondary structure. Although helices may rearrange in this process, the net change in helical content may not be large. Alternatively, it could also be that only a relatively small fraction of all t-SNAREs in the system actually bind VAMP2 to form the ternary complex, in which case the observed FTIR signals would still be dominated by uncomplexed t-SNAREs. More selective future experiments will be required to achieve a more detailed understanding of the molecular interactions that take place in the process of SNARE complex formation in a reconstituted membrane system.

Acknowledgment. This work was supported by National Institutes of Health Grant AI30577. We thank Drs. J. Rothman and T. Melia for supplying the recombinantly expressed syntaxin1A/SNAP-25 and VAMP2 proteins. Current members of the Tamm laboratory are gratefully acknowledged for many stimulating discussions and technical advice.

LA026228C

(41) Dulubova, I.; Sugita, S.; Hill, S.; Hosoka, M.; Fernandez, I.; Südhof, T. C.; Rizo, J. *EMBO J.* **1999**, *18*, 4372–4382.

(42) Xiao, W.; Poirier, M. A.; Bennett, M. K.; Shin, Y.-K. *Nat. Struct. Biol.* **2001**, *8*, 308–311.